eLIFE elifesciences.org

RESEARCH ARTICLE

Figures and figure supplements

Modeling of axonal endoplasmic reticulum network by spastic paraplegia proteins

Belgin Yalçın *et al*

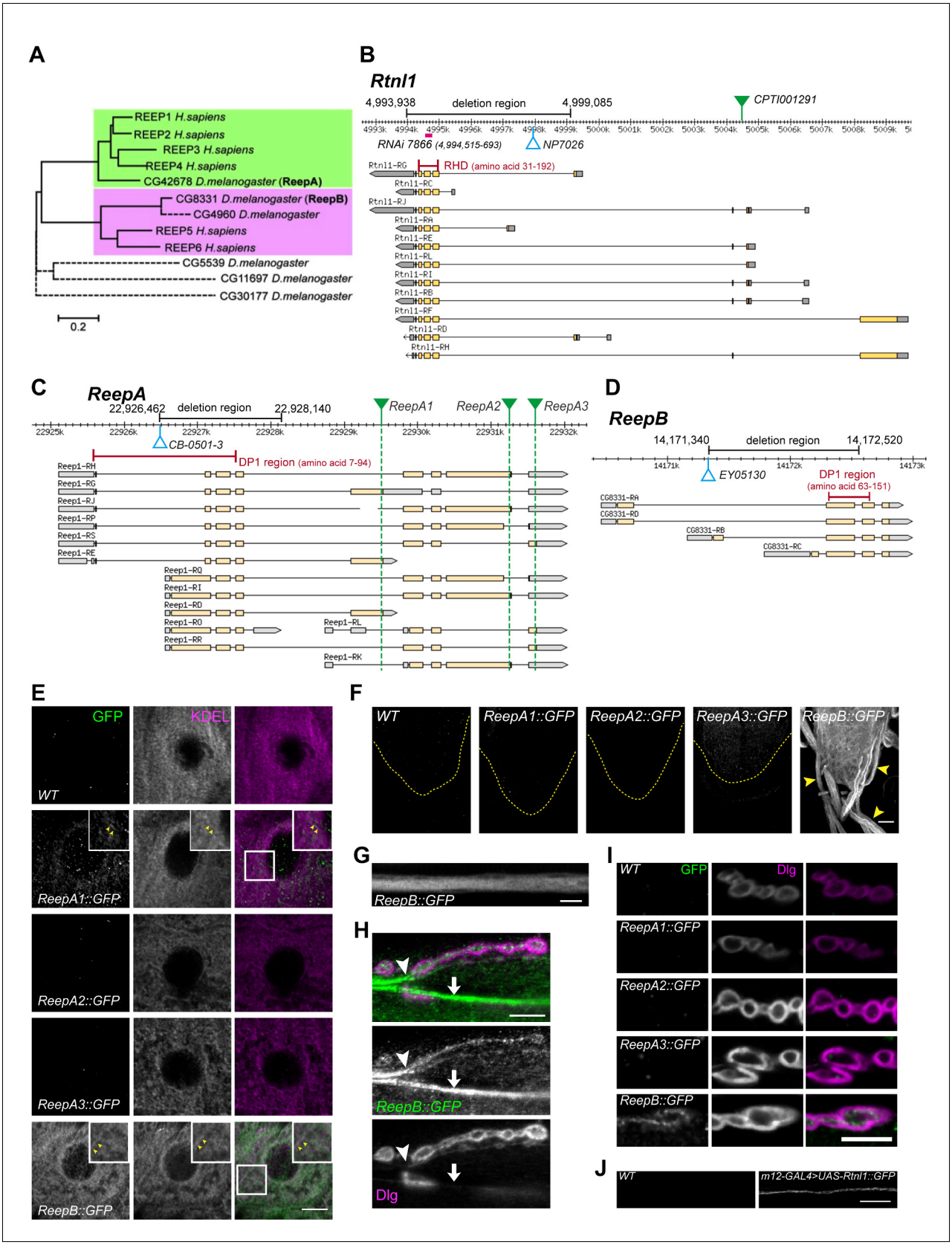

Figure 1. *Drosophila Rtnl1* and *REEP* genes and products. (**A**) A dendrogram based on ClustalW sequence alignment of *Drosophila* and human REEP proteins shows two branches corresponding to human REEP1-4 (CG42678) and human REEP5-6. Broken lines represent *Drosophila* REEP proteins that

Figure 1 continued on next page

Figure 1 continued

are evolving rapidly (***Supplementary file 1***), reflected by longer branch lengths. Sequences used are NP_075063.1, NP_057690.2, NP_001001330.1, NP_079508.2, NP_005660.4, NP_612402.1, NP_726266.1, NP_610936.2, NP_651429.1, NP_611831.2, NP_572730.1, NP_726366.1. (**B**) *Rtnl1* genomic and transcript map, showing the region deleted in *Rtnl1*$^{-}$ by excision of P-element *NP7026* (***Wakefield and Tear, 2006***; ***Figure 1—figure supplement 1***), the RHD domain (Pfam 02453) and its coordinates in protein isoform G, the Rtnl1::YFP exon trap insertion *CPTI001291* (green triangle), and the fragment targeted by GD RNAi 7866. Map and coordinates are from the *Drosophila* Genome Browser (www.flybase.org, version R6.04), here and in subsequent panels; light regions in transcripts represent coding regions, dark shaded regions represent untranslated regions. (**C**) *ReepA* genomic and transcript map showing the region deleted in *ReepA*$^{-}$ by excision of *P*-element *CB-0501–3*, the position of the DP1 domain (Pfam 03134) and its coordinates in protein isoforms H and J. GFP insertion sites for *ReepA1::GFP*, *ReepA2::GFP* and *ReepA3::GFP* fusions are shown with green triangles. (**D**) *ReepB* genomic and transcript map showing the region deleted in *ReepB*$^{-}$ by excision of *P*-element *EY05130*, the position of the DP1 domain (Pfam 03134) and its coordinates in protein isoforms A and D). (**E–I**) Confocal sections showing localization of ReepA::GFP isoforms and ReepB::GFP. (**E**) Overlap of ReepA1::GFP and ReepB::GFP with anti-KDEL labeling in larval epidermal cells. To facilitate display of weaker ReepA1::GFP, the GFP channel in wild-type control (*WT*) and *ReepA::GFP* images has been brightened four times as much as for *ReepB::GFP*. (**F**) Expression of ReepA3::GFP and ReepB::GFP in third instar ventral nerve cord. The GFP channels for *WT* and *ReepA::GFP* have been brightened by twice as much as for *ReepB::GFP*. VNCs are outlined with yellow dashed lines. Arrowheads show ReepB::GFP extending into peripheral nerves. (**G**) A single confocal section of a peripheral nerve, showing ReepB::GFP localized continuously along its length. (**H**) Double labeling of an NMJ for ReepB::GFP and the mainly postsynaptic marker Dlg, showing ReepB::GFP in an axon emerging from nerve bundles (arrowhead) to extend to the NMJ, as well as in axons traversing the muscle surface (arrow); note the dispersed ReepB::GFP staining also in the underlying muscle. (**I**) Double labeling of *ReepA::GFP* and *ReepB::GFP* lines for GFP and Dlg (mainly postsynaptic) shows presynaptic expression of ReepB::GFP. (**J**) GFP expression in a wildtype negative control (*WT*), or from Rtnl1::GFP expressed in two closely apposed motor neurons by *m12-GAL4*. Scale bars 10 μm, except F, 20 μm.

DOI: 10.7554/eLife.23882.003

A. *Rtnl1*[1] mutant sequence

```
GCGTCTATNTATCGTTTCTTCTTATTTCCCTCACTATATATGCTTTTTCCAAGGGAAATTCCGTTTCATTCGATTTTCAGCTGGCCATGCG
GTCGGCCCTCATATCTAGCCAAACCCTATATGTACATTTATATGAACATATA

>gnl|dmel|2L   type=golden_path_region; loc=2L:1..23513712; ID=2L; dbxref=GB:AE014134,
GB:AE014134, REFSEQ:NT_033779; length=23513712; release=r6.12;

Query:   15      TTTCTTCTTA-TTTCCCTCACTATATATGCTTTTT  48
                 |||||||||| |||||||||||||||||||||||
Subject: 4993903 TTTCTTCTTAATTTCCCTCACTATATATGCTTTTT  4993937

>gnl|dmel|2L   type=golden_path_region; loc=2L:1..23513712; ID=2L; dbxref=GB:AE014134,
GB:AE014134, REFSEQ:NT_033779; length=23513712; release=r6.12;

Query:   49      CCAAGGGAAATTCCGTTTCATTCGATTTTCAGCTGGCCATGCGGTCGGCCCTCATATCTA 108
                 ||||||||||||||||||||||||||||||||||||||||||||||||||||||||||||
Subject: 4999086 CCAAGGGAAATTCCGTTTCATTCGATTTTCAGCTGGCCATGCGGTCGGCCCTCATATCTA 4999145

Query:   109     GCCAAACCCTATATGTACATTTATATGAACATATA  143
                 |||||||||||||||||||||||||||||||||||
Subject: 4999146 GCCAAACCCTATATGTACATTTATATGAACATATA  4999180
```

B. *ReepA*[541] mutant sequence

```
TTCAATATCTTGATACTGAGGTGCTATTTTCTTGAACGCCTCTGTCGCAACATTCGGAACTGCGGCGCATTCCTACGTGTAAACCATGATG
AAATAACAAACAAACCCATGTCAAAGATCCCAGATACTCGCCGCAATTCACAACTGTTTTGTACACAATACAGATGTGGGCCAAGTCACTT
GTGGACTGCAACAGATTTTATGGCATCTGAAGTGCAGCAACCA

>gnl|dmel|2R   type=golden_path_region; loc=2R:1..25286936; ID=2R; dbxref=GB:AE013599,
GB:AE013599, REFSEQ:NT_033778; length=25286936; release=r6.12;

Query:   4         AATATCTTGATACTGAGGTGCTATTTTCTTGAACGCCTCTGTCGCAACATTCGGAACTGC 63
                  |||||||||||||||||||||||||||||||||||||||||||||||||||||||||||||
Subject: 22926381 AATATCTTGATACTGAGGTGCTATTTTCTTGAACGCCTCTGTCGCAACATTCGGAACTGC 22926440

Query:   64        GGCGCATTCCTACGTGTAAAC 84
                  |||||||||||||||||||||
Subject: 22926441 GGCGCATTCCTACGTGTAAAC 22926461

>gnl|dmel|2R   type=golden_path_region; loc=2R:1..25286936; ID=2R; dbxref=GB:AE013599,
GB:AE013599, REFSEQ:NT_033778; length=25286936; release=r6.12;

Query:   100       AACAAACCCATGTCAAAGATCCCAGATACTCGCCGCAATTCACAACTGTTTTGTACACAA 159
                  |||||||||||||||||||||||||||||||||||||||||||||||||||||||||||||
Subject: 22928141 AACAAACCCATGTCAAAGATCCCAGATACTCGCCGCAATTCACAACTGTTTTGTACACAA 22928200
```

C. *ReepB*[48] mutant sequence

```
TATTGAGACGTGGCGCTGTCGGCACACGTGGAGCCAATCTACTCACTCACCTGTGTGCGTTGGTAGAGCTTTCAGTTCGTTCCATGATGAA
ATAACATAGGTGAGCTTTGCATTCCTCACATATAAGAATCTTCTTTTAAATGCTTCAACTCCACATGTAGTGTGCTTTCCTCATCTGGTGC
ATGCTGCCCACGGAACAGAATGGTTCTACCATCATCTACA

>gnl|dmel|2R   type=golden_path_region; loc=2R:1..25286936; ID=2R; dbxref=GB:AE013599,
GB:AE013599, REFSEQ:NT_033778; length=25286936; release=r6.12;

Query:   1         TATTGAGACGTGGCGCTGTCGGCACACGTGGAGCCAATCTACTCACTCACCTGTGTGCGT 60
                  ||||||||||||||||||||||||||||||||||||||||||||||||||||||||||||
Subject: 14171258 TATTGAGACGTGGCGCTGTCGGCACACGTGGAGCCAATCTACTCACTCACCTGTGTGCGT 14171317

Query:   61        TGGTAGAGCTTTCAGTTCGTTC 82
                  |||||||||||||||||||||||
Subject: 14171318 TGGTAGAGCTTTCAGTTCGTTC 14171339

>gnl|dmel|2R   type=golden_path_region; loc=2R:1..25286936; ID=2R; dbxref=GB:AE013599,
GB:AE013599, REFSEQ:NT_033778; length=25286936; release=r6.12;

Query:   99        AGGTGAGCTTTGCATTCCTCACATATAAGAATCTTCTTTTAAATGCTTCAACTCCACATG 158
                  |||||||||||||||| |||||||||||||||||||||||||||||||||||||||||||
Subject: 14172521 AGGTGAGCTTTGCATTCTTCACATATAAGAATCTTCTTTTAAATGCTTCAACTCCACATG 14172580
```

Figure 1—figure supplement 1. Molecular lesions in *Rtnl1*[1], *ReepA*[541] and *ReepB*[48]. BLASTN searches of the *Drosophila* genome, using the sequences of (**A**) *Rtnl1*[1], (**B**) *ReepA*[541] and (**C**) *ReepB*[48] mutations as queries, show the coordinates of each molecular lesion in the genome, as gaps in alignments

Figure 1—figure supplement 1 continued on next page

Figure 1—figure supplement 1 continued

between mutant and genomic sequences. The *ReepA*^{541} and *ReepB*^{48} sequences highlighted in yellow show *P* element footprints left at the excision sites.

DOI: 10.7554/eLife.23882.004

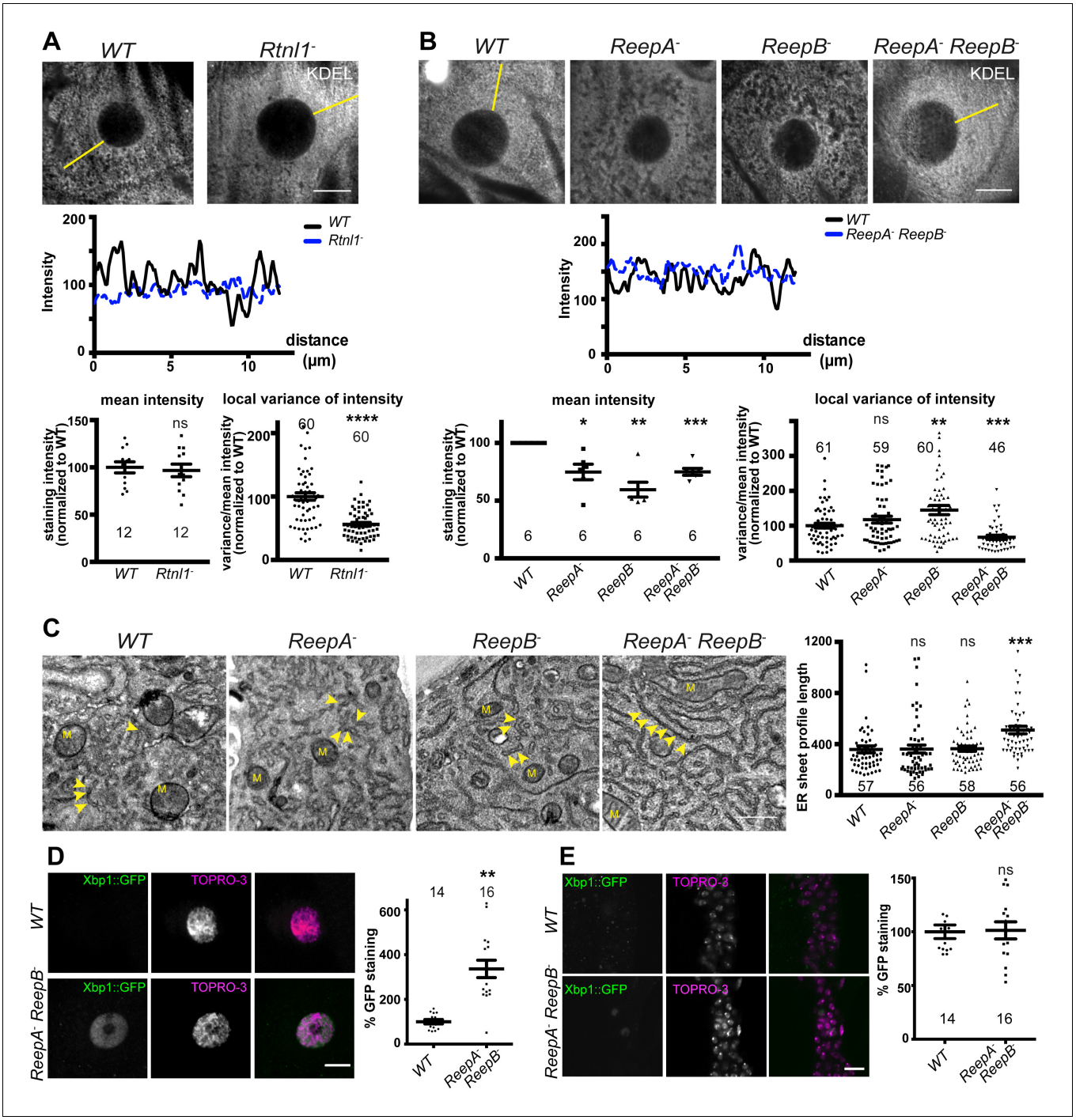

Figure 2. *Rtnl1*⁻ mutants and *ReepA*⁻ *ReepB*⁻ double mutants show disrupted ER organization in epidermal cells. (**A**) KDEL distribution in third instar larval epidermal cells appears diffuse in *Rtnl1*⁻ larvae compared to a more reticular staining in wild-type (*WT*) larvae. Micrographs show 1.5 µm z-projections of confocal sections. KDEL intensity along yellow lines from nuclear envelope to the cell periphery shows less fluctuation in *Rtnl1*⁻ (blue dotted line on line graph) than in *WT* larvae (black line on line graph). Fluctuation of intensity is quantified using the local normalized variance of intensity (variance/mean for rolling 10-pixel windows) over a 12 µm line for each cell. n = 61 epidermal cells from 12 larvae, 3–5 cells from each larva, from 3 independent experiments. (**B**) KDEL distribution in third instar larval epidermal cells shows less spatial fluctuation in *ReepA*⁻ *ReepB*⁻ double mutant larvae compared to *ReepA*⁺ (*WT*), and *ReepA*⁻ and *ReepB*⁻ single mutant larvae. This is confirmed by quantification as in **A**); overall KDEL intensity is reduced in all ReepA and ReepB mutant genotypes. n = 45–61 epidermal cells in total from 12 to 16 different larvae, 3–5 cells from each larva, from 6 independent experiments. Intensity datapoints are experimentwise averages of multiple larvae, compared by paired t-tests, since larva-wise data were too significantly different to pool across experiments in this case. (**C**) Electron micrographs show increased ER sheet profile length in

Figure 2 continued on next page

Figure 2 continued

ReepA^{-} *ReepB*$^{-}$ double mutant third instar larval epidermal cells compared to single *ReepA*$^{-}$ and *ReepB*$^{-}$ mutants and controls. Arrowheads, ER sheets; M, mitochondria. (n = 56–58 cells in total from three independent larvae, 18–19 cells from each. (**D**,**E**) *ReepA*$^{-}$ *ReepB*$^{-}$ double mutant larvae have an increased ER stress response compared to a *ReepA*$^{+}$ (*WT*) control, measured by Xbp1::GFP expression, in larval epidermis (**D**) but not in neuronal cell bodies (**E**). Graphs show quantification of Xbp1::GFP staining intensity relative to controls. (n = 12–15 larvae). All graphs show individual datapoints and mean ±SEM. Occasional outlier datapoints off the top of the scale are omitted from graphs but included in statistical analyses. ns, p>0.05; *p<0.02; **p<0.005; ***p<0.0003; ****p<0.0001, two-tailed Student's t-test. Scale bars: A, B, D, E, 10 μm; C, 0.5 μm).

DOI: 10.7554/eLife.23882.005

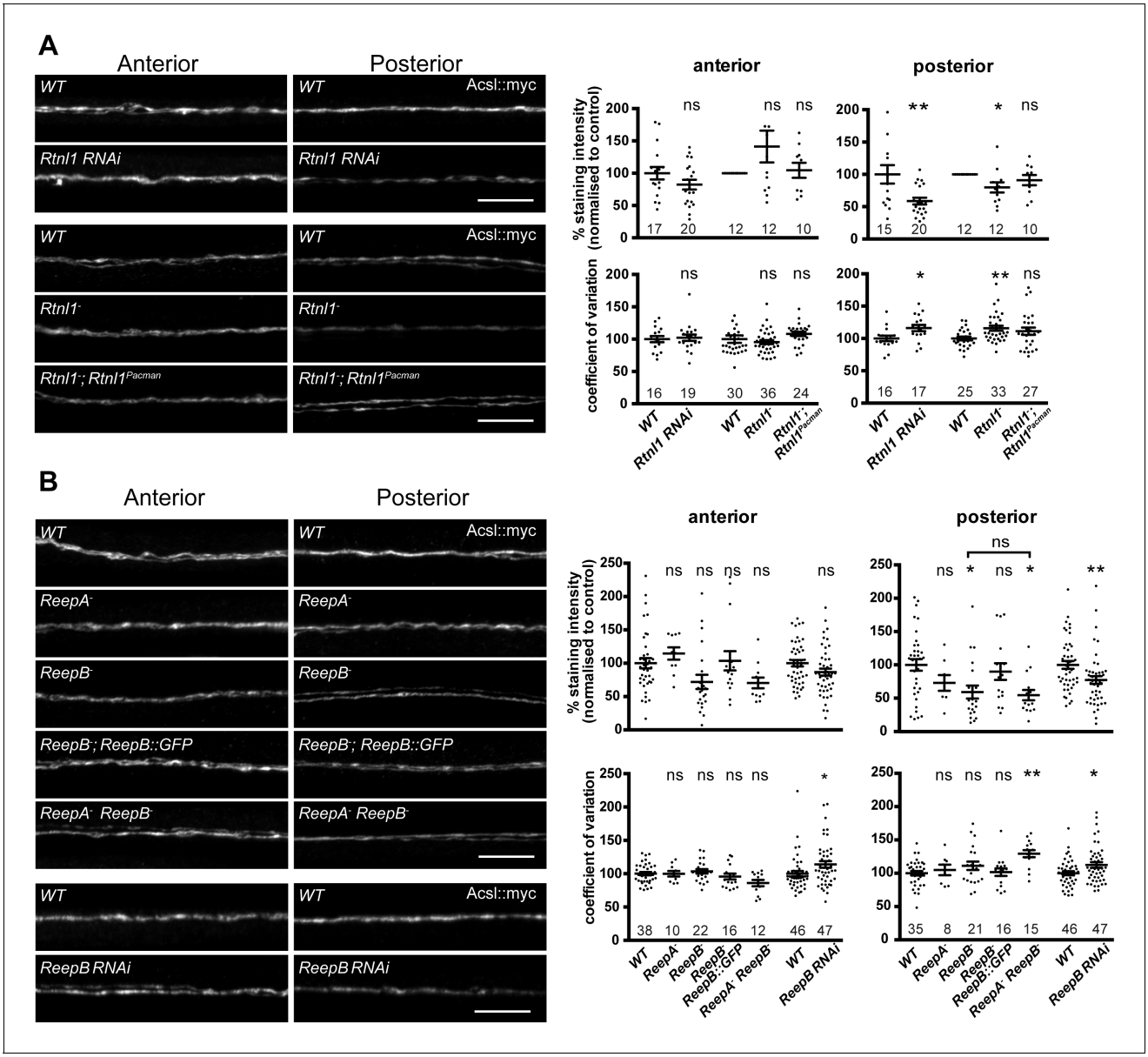

Figure 3. Loss of either Rtnl1 or ReepB leads to partial loss of smooth ER marker from distal motor axons. (**A**) Effects of Rtnl1 loss on ER, visualized by Acsl::myc expressed in two adjacent motor axons using *m12-GAL4*. Images show effects of *Rtnl1* knockdown, *Rtnl1*$^{-}$ mutation, rescue of *Rtnl1*$^{-}$ by *Rtnl1*^{Pacman} and respective *ReepA*$^{+}$ control (*WT*) axons. Graphs show mean staining intensity (top graphs) or coefficient of variation of intensity (bottom graphs) as a measurement of staining variability along the length of each axon. Rtnl1 loss leads to partial loss of Acsl::myc in posterior but not anterior axons (top graphs), and to some disorganization of posterior axonal ER seen by increased coefficient of variation of Acsl::myc staining intensity. There is partial rescue of *Rtnl1* phenotypes by one copy of a *Rtnl1*^{Pacman} genomic clone. n = 15–20 larvae per genotype pooled from 5 independent experiments for RNAi; n = 24–36 larvae per genotype from 10 to 12 independent experiments for *Rtnl1*$^{-}$ mutant. Graphs show individual datapoints with mean ±SEM; ns, p>0.05; *p<0.03; **p<0.005; two-tailed unpaired Student's t-test; two-tailed paired Student's t-test was used when larva-wise data were too significantly different across experiments (p<0.05, ANOVA) to pool. (**B**) Effects of ReepA or ReepB loss on axonal ER. *ReepB* knockdown or *ReepB*$^{-}$ mutation, but not *ReepA* mutation, causes partial loss of smooth ER marker Acsl::myc in posterior but not in anterior motor axons. The *ReepB*$^{-}$ phenotype can be mostly rescued by one copy of a genomic *ReepB::GFP* clone. A *ReepA*$^{-}$ *ReepB*$^{-}$ double mutant shows a similar phenotype to a *ReepB*$^{-}$ single mutant. *ReepA*$^{-}$ *ReepB*$^{-}$ double mutant, but not single *ReepA*$^{-}$ or *ReepB*$^{-}$ mutants, show increased coefficient of variation of Acsl::myc staining levels in posterior axons; n = 7–47 larvae from 4 to 11 independent experiments. All graphs show individual datapoints with mean ±SEM; occasional outlier datapoints off the top of the scale are omitted from graphs but included in statistical analyses. ns, p>0.05; *p<0.04 **p<0.01. *ReepB* RNAi was analyzed using two-tailed unpaired Student's t-tests; multiple comparisons of *ReepA* and *ReepB* mutant genotypes were analyzed by ANOVA followed by post-hoc Tukey HSD tests. Scale bars, 10 μm.

DOI: 10.7554/eLife.23882.006

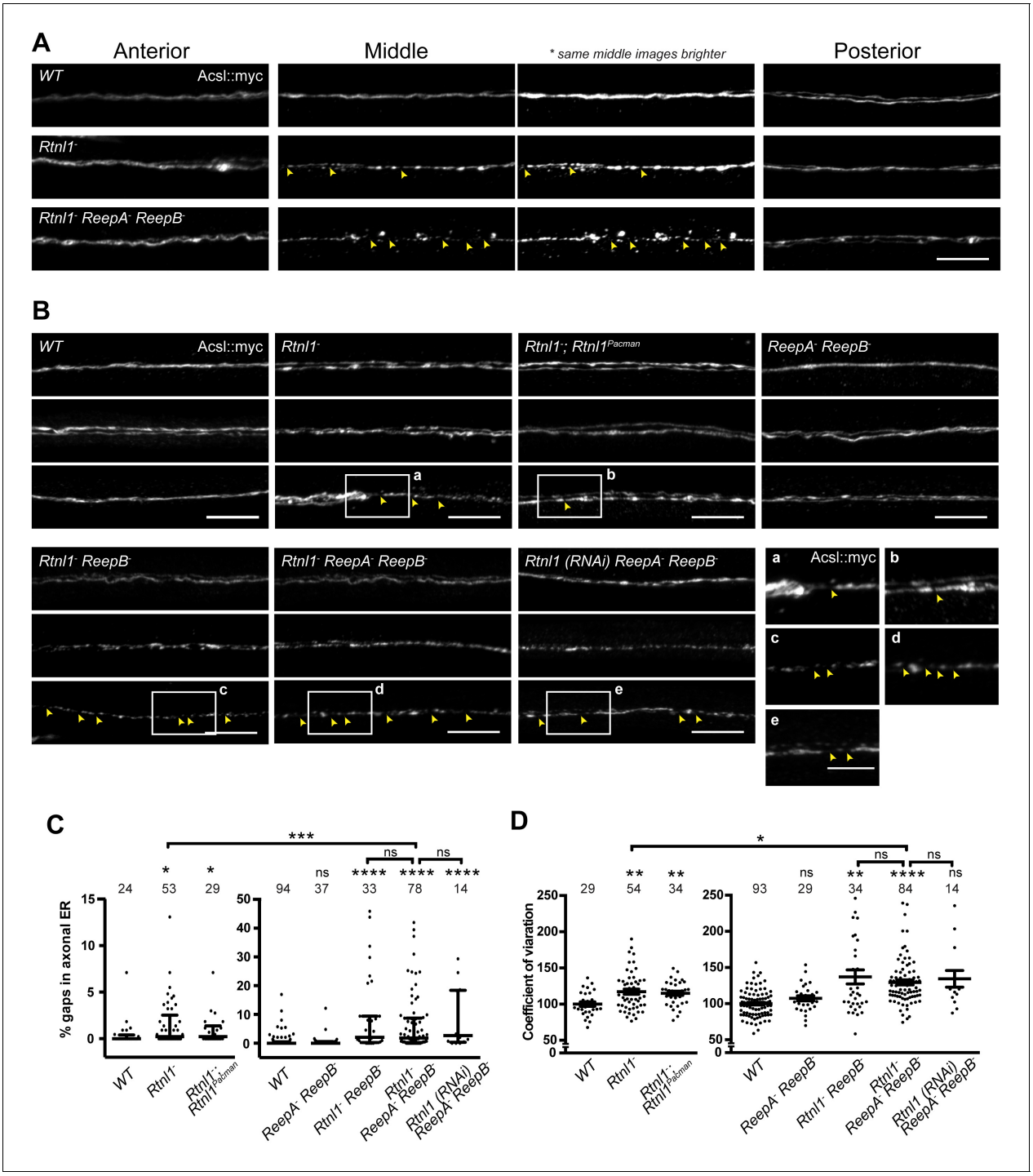

Figure 4. Loss of hairpin proteins leads to discontinuity of axonal ER staining. (**A**) *Rtnl1*$^{-}$ larvae and *Rtnl1*$^{-}$ *ReepA*$^{-}$ *ReepB*$^{-}$ triple mutant larvae sometimes show fragmented axonal ER labeling in the middle parts (segment A5) of long motor axons that express Acsl::myc under control of *m12-GAL4*. Anterior (segment A2) and posterior (segment A6) portions of the same motor axons show continuous ER labeling. Arrowheads show gaps in Acsl::myc staining; brighter versions of the same images show gaps in staining in mutants but not wild-type (*WT*), even when brightness of remaining staining is saturating. (**B**) Panels show three examples of the range of Acsl::myc distributions found in the middle parts of long motor axons of each genotype of *ReepA*$^{+}$ (*WT*), *Rtnl1*$^{-}$, *Rtnl1*$^{-}$ rescued with a *Rtnl1*^{Pacman} construct, *ReepA*$^{-}$ *ReepB*$^{-}$ and *Rtnl1*$^{-}$ *ReepB*$^{-}$ double mutants, *Rtnl1*$^{-}$ *ReepA*$^{-}$ *ReepB*$^{-}$ triple mutant, and *Rtnl1(RNAi) ReepA*$^{-}$ *ReepB*$^{-}$ larvae. A variety of phenotypes, from continuous to fragmented Acsl::myc labeling, are found in genotypes that lack Rtnl1, and tend to be more severe in genotypes that also lack ReepB. Insets show examples of gaps in ER continuity (arrowheads) at higher magnification. Scale bars 10 μm, and 5 μm in higher zoom images. (**C**) Percentages of a 45 μm length in the middle (A4/A5 segment) of each axon that lacks Acsl::myc staining, using an intensity threshold of 20 on a scale of 0–255. Individual axons are plotted, together with median and

Figure 4 continued on next page

Figure 4 continued

interquartile range; comparisons use Mann-Whitney U-tests. All genotypes that lack Rtnl1 show more gaps than *WT*; *Rtnl1*$^{-}$ *ReepA*$^{-}$ *ReepB*$^{-}$ triple mutants do not differ from *Rtnl1(RNAi) ReepA*$^{-}$ *ReepB*$^{-}$ or *Rtnl1*$^{-}$ *ReepB*$^{-}$ double mutants, but are significantly more severe than *Rtnl1*$^{-}$ single mutants. (**D**) The coefficient of variation of Acsl::myc labeling in middle axon portions is increased in genotypes lacking Rtnl1, relative to controls. Graphs show individual datapoints with mean ±SEM; occasional outlier datapoints off the top of the scale are omitted from graphs but included in statistical analyses. Comparison between *Rtnl1*$^{-}$ and *Rtnl1*$^{-}$ *ReepA*$^{-}$ *ReepB*$^{-}$ mutant genotypes was analyzed by two-tailed Student's t-test, other multiple comparisons by ANOVA followed by Dunnett's T3 test. ns, $p>0.05$; *$p<0.04$; **$p<0.01$; ***$p<0.0005$; ****$p<0.0001$; individual axons are plotted from 3 to 20 independent experiments, each with 2–3 different larvae for each genotype.

DOI: 10.7554/eLife.23882.007

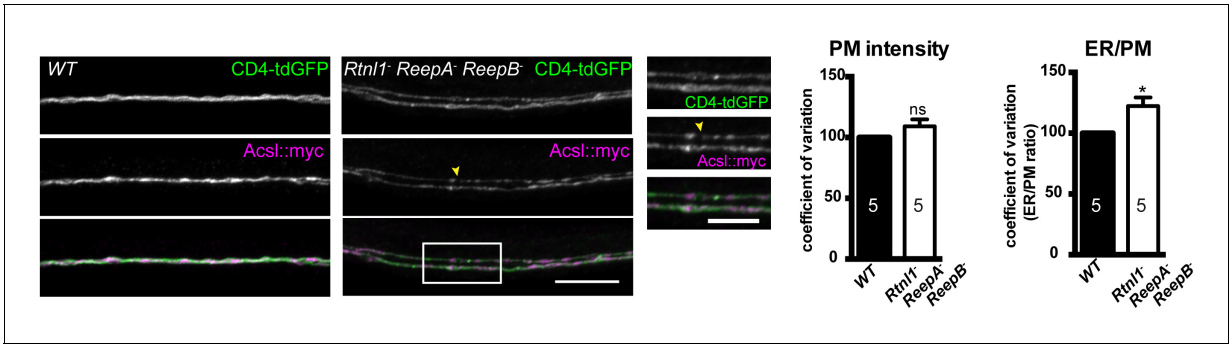

Figure 4—figure supplement 1. Plasma membrane integrity is not affected in *Rtnl1*$^{-}$ *ReepA*$^{-}$ *ReepB*$^{-}$ triple mutant larvae). Coefficient of variation for plasma membrane labeling along axon length is unchanged in *Rtnl1*$^{-}$ *ReepA*$^{-}$ *ReepB*$^{-}$ triple mutant compared to control (*WT*) axons, whereas the ER to plasma membrane ratio of the coefficient of variation is increased. Higher zoom images of the boxed areas show gaps (yellow arrowheads) and brightly labeled axonal ER accumulations. Graphs show mean ±SEM; *p<0.02, two-tailed Student's t-test; n = 5 different larvae from 3 independent experiments.

DOI: 10.7554/eLife.23882.008

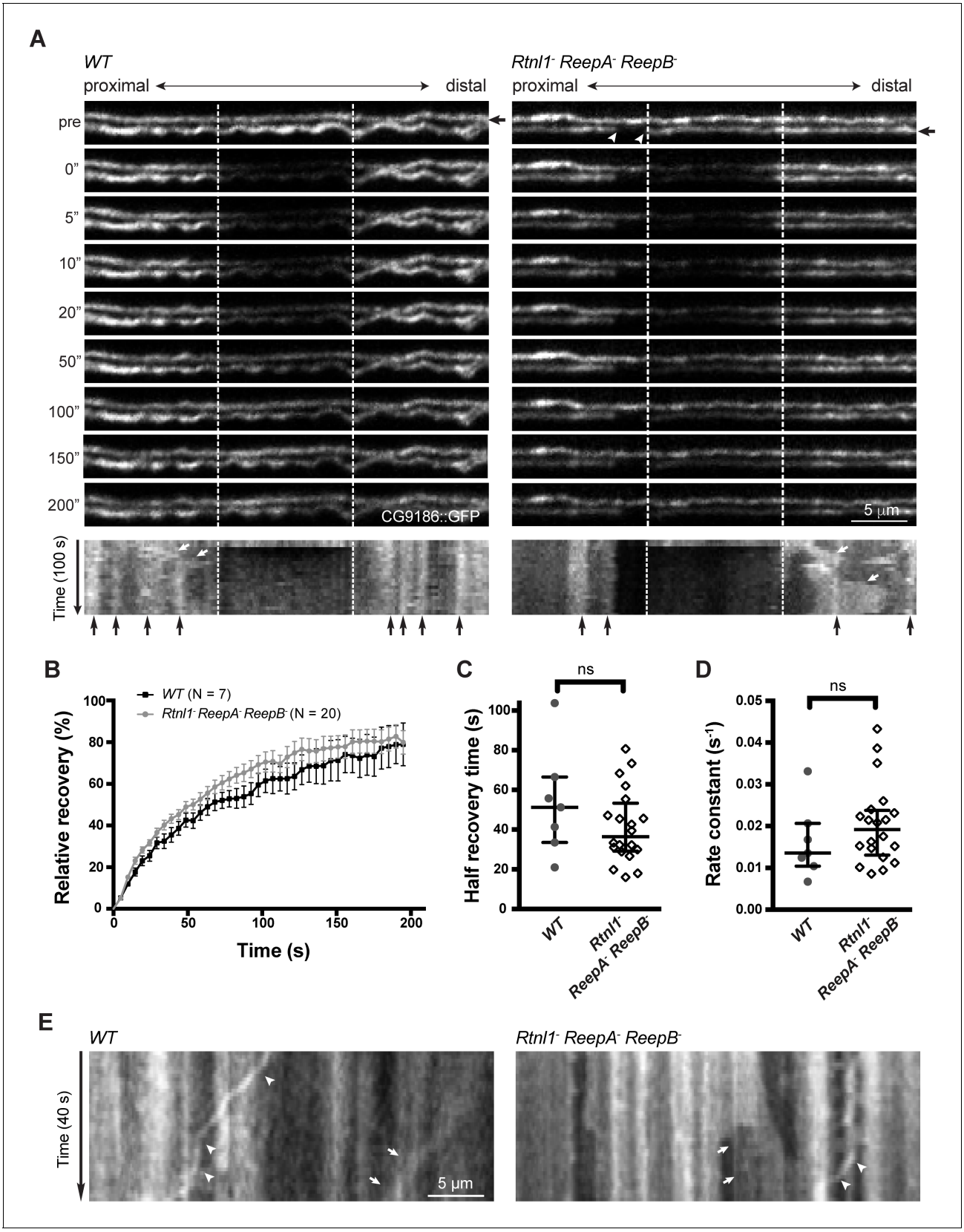

Figure 5. Live imaging of ER in wild type and hairpin mutant axons. (**A**) Representative FRAP assay images from *ReepA*$^{+}$ (*WT*) or *Rtnl1*$^{-}$ *ReepA*$^{-}$ *ReepB*$^{-}$ triple mutant axons in which ER was visualized using CG9186::GFP expression driven in two motor axons by *m12-GAL4*. One triple mutant axon

Figure 5 continued on next page

Figure 5 continued

shows a gap in labeling (arrowheads). Regions of interest (12 µm, between dashed lines) were photobleached. Fluorescence was visualized before photobleaching ('pre'), and during recovery over 200 s. A kymograph was generated for each axon indicated by an arrow in the top panel. Most areas of intense and less intense ER labeling remain stable over time (e.g. black arrows below kymographs); occasional movements of ER features are indicated by white arrows in kymographs. (**B**) Relative fluorescence intensities within the photobleached region were plotted (mean ±SEM) during recovery for wild-type axons or for triple mutant axons lacking ER gaps. (**C–D**) Quantification of half recovery time (**C**) and rate constant (**D**) for wild-type and triple mutant axons lacking gaps, with median and interquartile range. Data in **B–D** are from seven recordings from 4 wild-type larvae, and 20 recordings from 14 mutant larvae. ns, p>0.05; Mann-Whitney U test. Scale bars, 5 µm. (**E**) Representative kymographs from time-lapse recording of CG9186::GFP in unbleached single *ReepA*$^{+}$ (*WT*) or *Rtnl1*$^{-}$ *ReepA*$^{-}$ *ReepB*$^{-}$ triple mutant axons lacking gaps. The left panel shows retrograde movement of a ~ 3 µm length of ER labeling (arrows); the right panel shows anterograde movement of a ~ 5 µm stretch of ER labeling (arrows). Retrograde movements of labeled puncta are seen in both panels (arrowheads).

DOI: 10.7554/eLife.23882.009

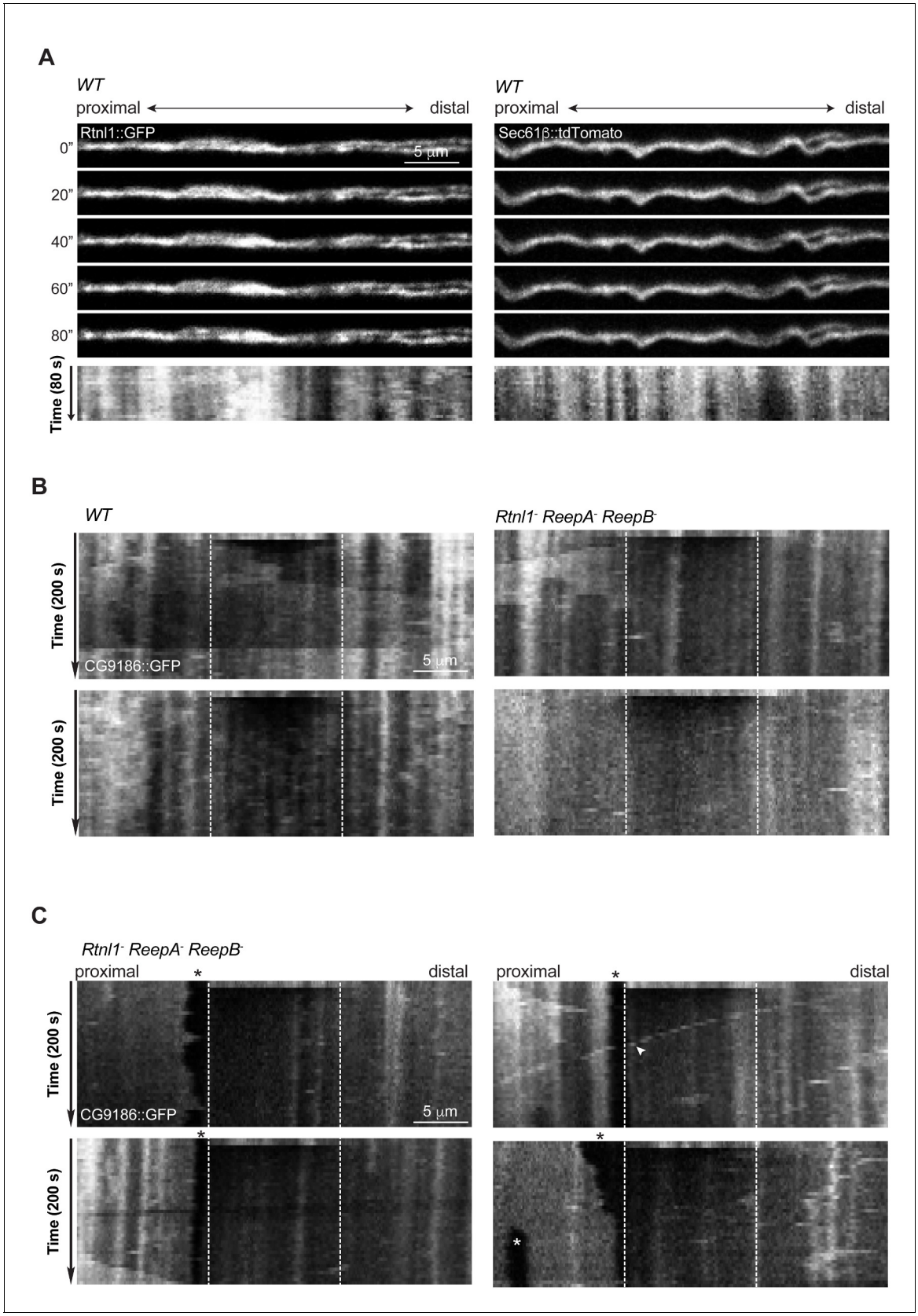

Figure 5—figure supplement 1. Continuity, stability and movement of fluorescent ER labeling in wild-type (*WT*) and *Rtnl1*$^{-}$ *ReepA*$^{-}$ *ReepB*$^{-}$ triple mutant axons. (**A**) Time series and kymographs of two closely apposed motor axons expressing either Rtnl1::GFP or Sec61b*β*::tdTomato ER markers

Figure 5—figure supplement 1 continued on next page

Figure 5—figure supplement 1 continued

under control of *m12-GAL4*. Images show continuity of ER staining in axons, and kymographs show stability of most ER features over the acquisition time. (**B**) Kymographs showing fluorescence recovery after photobleaching in two *ReepA*$^{+}$ (*WT*) axons, or in two *Rtnl1*$^{-}$ *ReepA*$^{-}$ *ReepB*$^{-}$ triple mutant axons lacking ER gaps. Recovery proceeds from both ends of the bleached region (dotted lines). Most ER features seen before bleaching (top line of kymographs) can also be seen after recovery, implying that recovery proceeds by protein diffusion, not by movement of ER structures. (**C**) Kymographs showing fluorescence recovery after photobleaching immediately distal to gaps in ER staining, in four *Rtnl1*$^{-}$ *ReepA*$^{-}$ *ReepB*$^{-}$ triple mutant axons. Recovery proceeds only from the distal end of the bleached region (dotted lines) opposite the gap, but not across the proximal gap. While most ER gaps and many other features are stable, one axon shows a retrogradely moving particle (white arrowhead), and one shows anterograde movement of ER that closes one gap and opens another more proximally (white asterisk).

DOI: 10.7554/eLife.23882.010

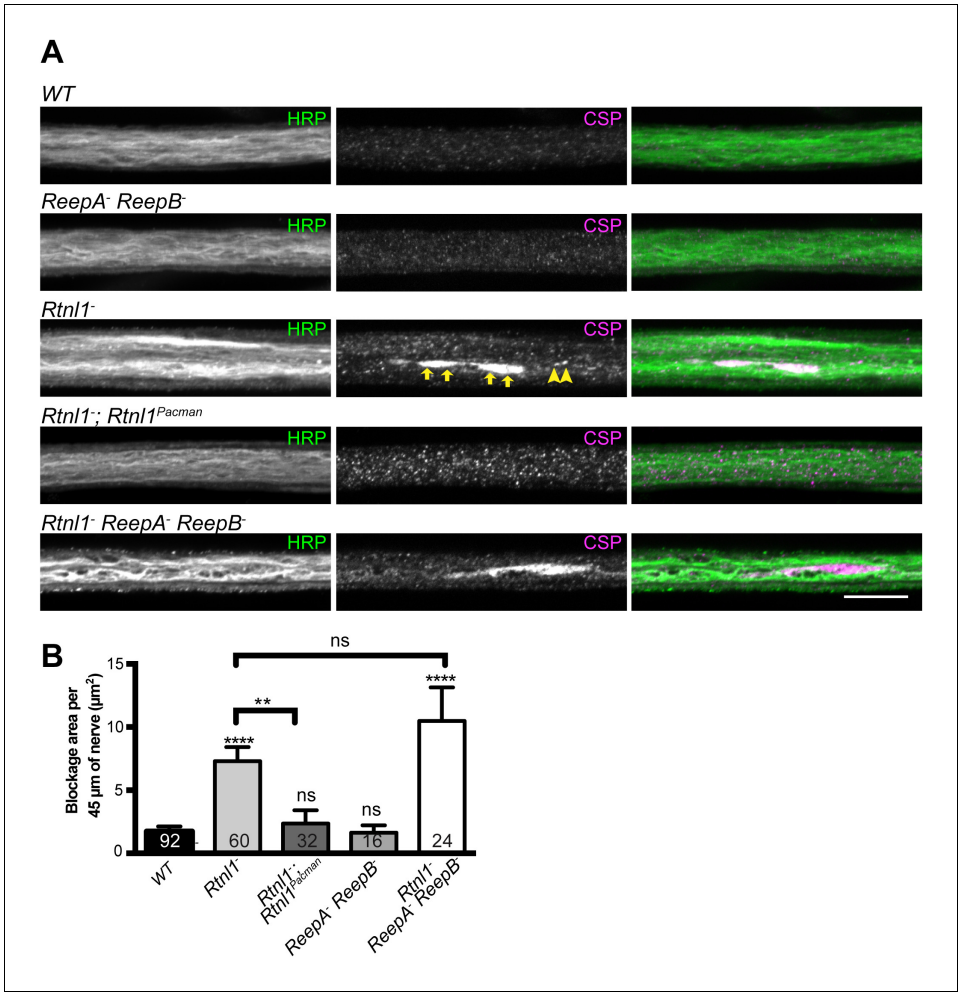

Figure 6. Loss of Rtnl1 causes mild accumulation of synaptic vesicles in axons. (**A**) Peripheral nerves of *Rtnl1*$^{-}$ and *Rtnl1*$^{-}$ *ReepA*$^{-}$ *ReepB*$^{-}$ triple mutant larvae show larger accumulations of synaptic vesicle protein CSP (e.g. yellow arrows), and smaller elongated CSP puncta (e.g. yellow arrowheads). In contrast, control larvae (*WT*) and *ReepA*$^{-}$ *ReepB*$^{-}$ double mutant larvae show an even distribution of small round CSP puncta. CSP accumulations are not significantly bigger in *Rtnl1*$^{-}$ *ReepA*$^{-}$ *ReepB*$^{-}$ triple mutants than in *Rtnl1*$^{-}$ mutants. The CSP accumulations in *Rtnl1*$^{-}$ larvae can be rescued by two copies of a *Rtnl1*^{Pacman} genomic clone. All axons shown are crossing abdominal segment A2. (**B**) Graph shows mean ±SEM; n = 16–92 axons from 8 to 46 larvae, from 3 different experiments. ns, p>0.05; **p<0.006; ****p<0.0001, two-tailed Student's t-test. Scale bar, 10 µm).
DOI: 10.7554/eLife.23882.015

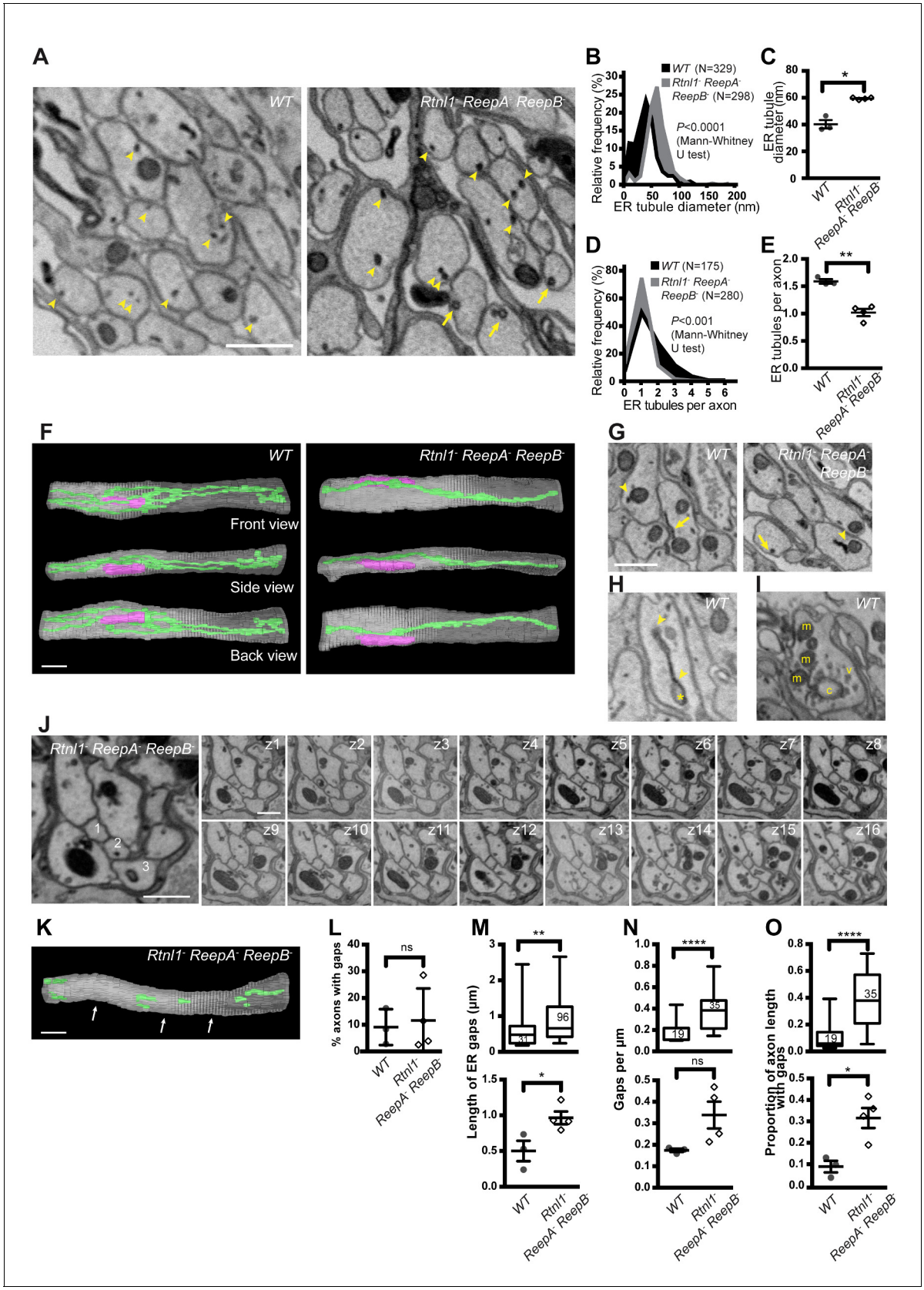

Figure 7. Loss of hairpin proteins leads to fewer but enlarged ER tubules in larval peripheral nerve axons. (**A**) EMs of peripheral nerve axons from wild-type *ReepA*$^{+}$ (*WT*, left) or *Rtnl1*$^{-}$ *ReepA*$^{-}$ *ReepB*$^{-}$ triple mutant (right) larvae. Arrowheads indicate ER tubules (seen as continuous structures in serial

Figure 7 continued on next page

Figure 7 continued

sections in ***Videos 5*** and ***7***). Triple mutant axons show enlarged ER tubules, sometimes with a clear lumen (arrows), seldom observed in wild-type. Quantification of ER tubule diameter (**B,C**) and tubules per axon cross-section (**D,E**) in control and mutant larvae. Data from individual ER tubules or axons are shown in B and D, averaged larval values, mean ±SEM in C and E. (**F**) 3D reconstruction of a 4.5 µm axon segment from wild-type (left) or mutant (right) peripheral nerves, generated from 75 serial 60 nm sections, showing ER (green), mitochondria (magenta) and plasma membrane (gray). Interactive versions of the reconstructions are in ***Supplementary files 2*** and ***3***. (**G**) Electron micrographs of peripheral nerve axons from wild-type (*ReepA*$^{+}$, left) or *Rtnl1*$^{-}$ *ReepA*$^{-}$ *ReepB*$^{-}$ triple mutant (right) larvae, showing proximity of ER to mitochondria (arrowheads) or plasma membrane (arrows). (**H**) Representative EM of short ER sheet (arrowhead) and cisterna (asterisk) from a wild-type larva; further sections in ***Video 6***. (**I**) section of an axonal swelling from a wild-type larva showing mitochondria (m), vesicles (v), and a large clear cisterna (c); further sections in ***Video 8***. (**J**) Serial EM sections show ER discontinuity in two mutant axons: axon 1 lacks ER tubules in sections z6-z14 and axon 3 in sections z1-z11; neighboring axons (e.g. axon 2) show a continuous ER network. (**K**) 3D reconstruction of a 4.5 µm axon segment from mutant peripheral nerves, generated from 75 serial 60 nm sections, showing multiple gaps (indicated by arrows). ER is in green and plasma membrane in gray. Raw EM data and an interactive version of the reconstruction are in ***Video 9*** and ***Supplementary file 4***, respectively. (**L**) Frequency of axons with gaps in the 4.5 µm lengths analyzed. ER gap length (**M**), numbers of ER gaps per µm (**N**), and proportion of axon length with gaps (**O**) in affected axons. In **M–O**, top graphs show data from individual ER gaps (**M**) or individual axons (**N–O**), with second and third quartiles and 5th and 95th percentiles; bottom graphs show averaged larval values, mean ±SEM. In all graphs, ns p>0.05; *p<0.04; **p<0.003; ****p<0.0001; Mann-Whitney U test for **B**, **D**, top graphs in **M–O**; two-tailed Student's T test for **C**, **E**, **L**, bottom graphs in **M–O**. Scale bars, 500 nm.

DOI: 10.7554/eLife.23882.016

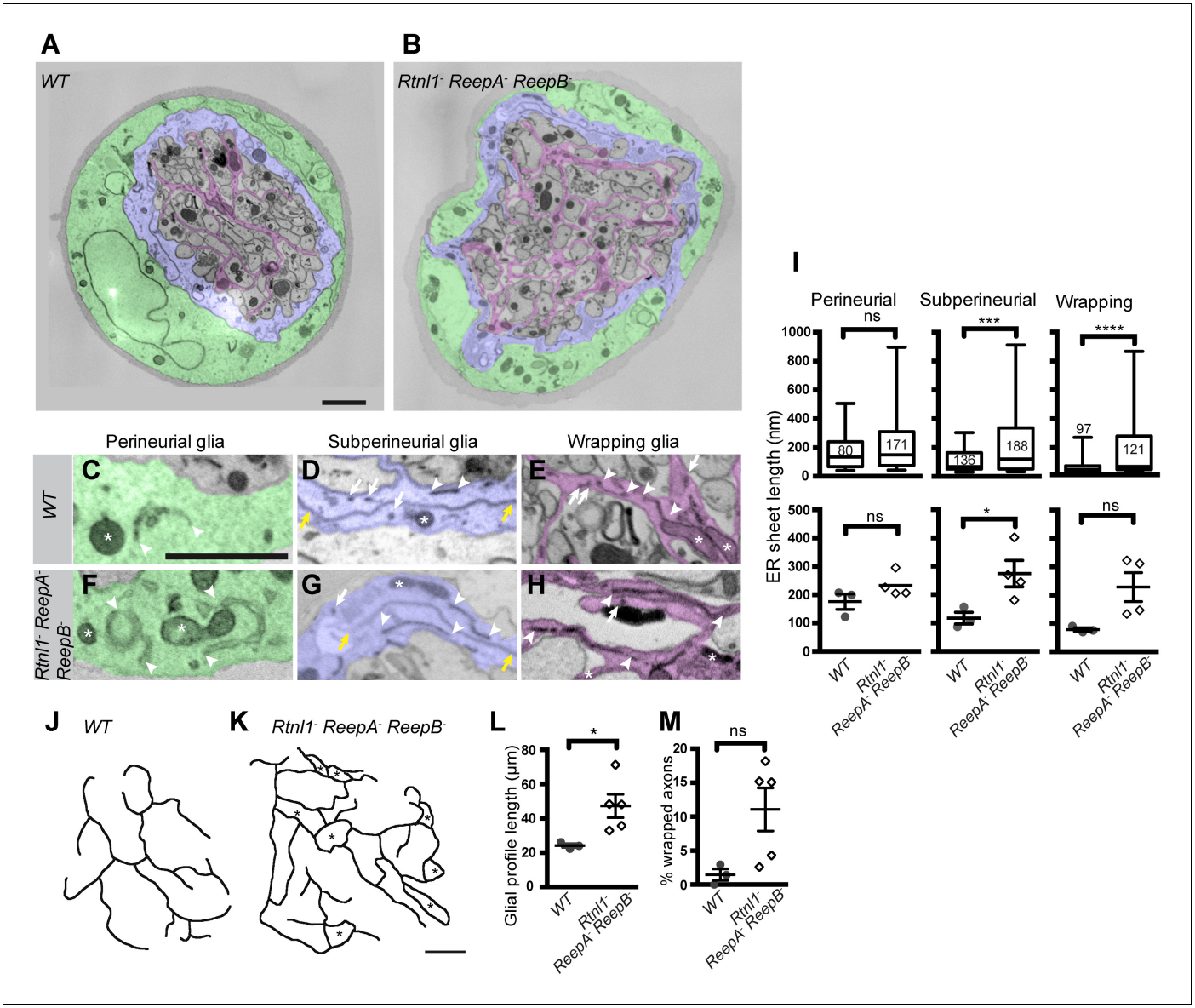

Figure 8. Loss of reticulon and REEP proteins leads to ER disorganization in glial cells and hyper-wrapping of peripheral axons. (**A–B**) EMs of peripheral nerve sections from *ReepA*$^{+}$ (*WT*) (**A**) or *Rtnl1*$^{-}$ *ReepA*$^{-}$ *ReepB*$^{-}$ triple mutant (**B**) larvae. Perineurial, subperineurial, and wrapping glial cells are shaded green, blue, and magenta, respectively. (**C–H**) Higher magnification images of perineurial (**C**,**F**), subperineurial (**D**,**G**), and wrapping (**E**,**H**) glia from wild-type (**C–E**) or mutant (**F–H**) nerve sections, showing ER tubules (white arrows; confirmed as tubules by presence in adjacent sections) and sheets (white arrowheads). Note the longer ER sheet profiles and fewer ER tubules in the subperineurial (**G**) and wrapping glial cells (**H**) of mutant nerves. Asterisks show mitochondria; yellow arrowheads show glial plasma membrane, identified by its continuity. (**I**) ER sheet profile length in control and mutant glial cells from 3 wild-type and 4 mutant larvae. Top graphs represent all individual sheet profiles, with second and third quartiles and 5th and 95th percentiles; bottom graphs show averaged larval values, showing mean ±SEM. Two-way ANOVA showed a significant effect of genotype ($p<0.002$) but not glial class ($p>0.3$) on ER sheet length, with no interaction between factors ($p>0.3$). (**J**,**K**) Sketches of wild-type (**J**) and mutant (**K**) wrapping glial cells, showing excess processes in the triple mutant. Asterisks indicate completely wrapped one-axon or two-axon fascicles, rarely seen in wild-type nerve sections. More examples of each phenotype are in ***Figure 8—figure supplement 1***. (**L–M**) Quantification of wrapping glial membrane profile length per nerve cross-section (**L**) and percentage of axons that are wrapped individually or as two-axon fascicles (**M**) in wild-type and mutant nerve sections (mean ±SEM). ns, $p>0.05$; *$p<0.05$; ***$p<0.001$; ****$p<0.0001$. Mann-Whitney U test (**I**), top graphs); two-tailed Student's t-test (**I**), bottom graphs; **L**, **M**,). Scale bars, 1 µm.

DOI: 10.7554/eLife.23882.022

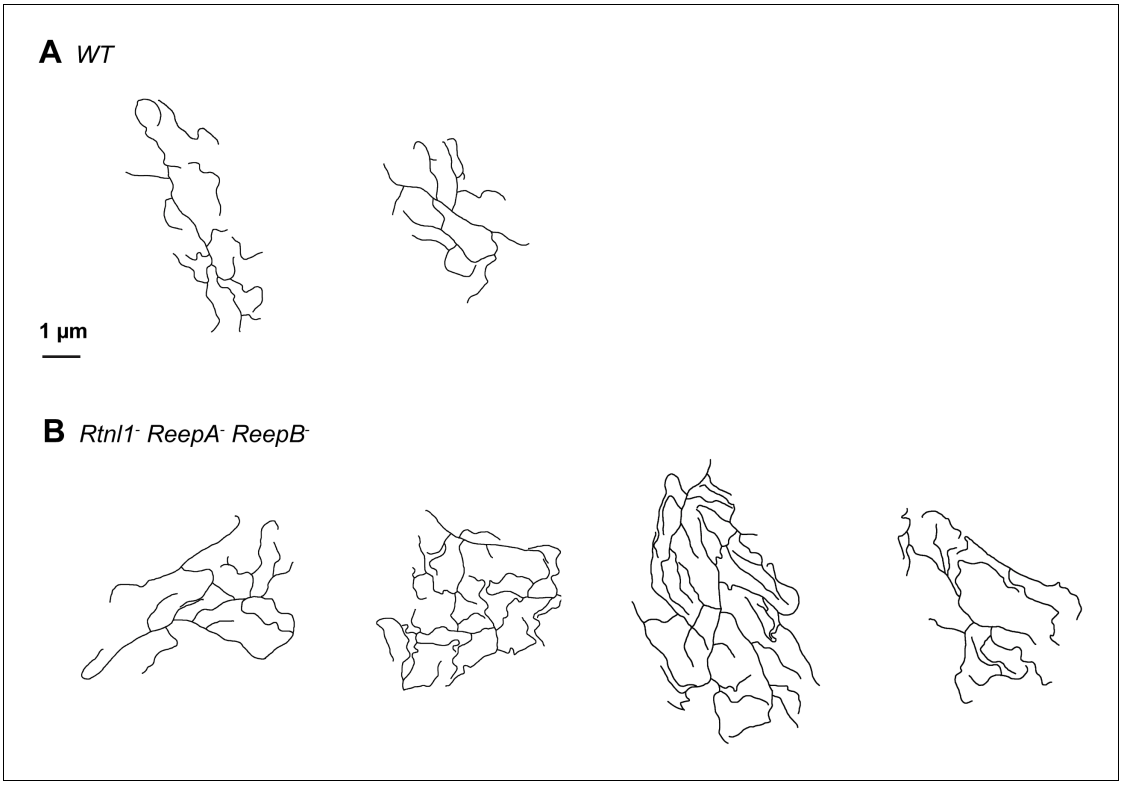

Figure 8—figure supplement 1. Sketches of wrapping glia in wild-type (*ReepA*$^{+}$) and *Rtnl1*$^{-}$ *ReepA*$^{-}$ *ReepB*$^{-}$ mutant peripheral nerves, similar to those in ***Figure 8J,K***. Sketches of wild-type (*ReepA*$^{+}$, upper) and mutant (lower) wrapping glial cells were abstracted from cross-sections of peripheral nerves. Excess formation of processes were observed in triple mutants.

DOI: 10.7554/eLife.23882.023